



Proceedings of the Sixth International Conference on  
Railway Technology: Research, Development and Maintenance  
Edited by: J. Pombo  
Civil-Comp Conferences, Volume 7, Paper 2.2  
Civil-Comp Press, Edinburgh, United Kingdom, 2024  
ISSN: 2753-3239, doi: 10.4203/ccc.7.2.2  
©Civil-Comp Ltd, Edinburgh, UK, 2024

# The Effect of Loading Configuration on the Slipstream of Freight Trains

J. Bell<sup>1</sup>, A. Buhr<sup>1</sup>, L. Siegel<sup>1</sup>, R. Volkert<sup>2</sup>, O. Michael<sup>3</sup>,  
C. Renschler<sup>4</sup> and A. Henning<sup>1</sup>

<sup>1</sup>Institute of Aerodynamics and Flow Technology, German Aerospace Center  
Göttingen, Germany

<sup>2</sup>Aerodynamics and Air Conditioning, DB Systemtechnik GmbH, Munich,  
Germany

<sup>3</sup>Technical Management Wagons, DB Cargo AG, Minden, Germany

<sup>4</sup>Product Management Intermodal Sales, DB Cargo AG, Mainz, Germany

## Abstract

The slipstream of freight trains was investigated using two experimental aerodynamic methodologies: a scaled wind-tunnel and scaled moving-model. Both experimental methodologies identified the large effect loading configuration can have on slipstream, with container sized gaps having the largest effect, whilst wagon-wagon sized gaps were also identified as having potential for optimisation. Gap order was also identified as having an influence. Additional insight into the cause of the peak slipstream was achieved with flow field measurements using particle image velocimetry.

**Keywords:** slipstream, freight train, transient flow, induced flow, aerodynamics, loading configuration

## 1 Introduction

Slipstream – the flow induced by a train’s movement through the air – is an important aerodynamic characteristic of trains, that can affect the safety of commuters and trackside workers, as well as being a damage concern for trackside infrastructure [1,2]. The slipstream of high-speed passenger trains at travelling speeds of ~250 km/h can reach average velocities of ~40 km/h (~15% of the train speed) typically behind the train, with significantly larger instantaneous peaks. The causes of slipstream have been well researched and proposed to be caused by transient coherent structures in the wake of the train [3]. In comparison, the average slipstream of freight trains travelling

at ~110 km/h have been found to be ~33 km/h, (30% of the train speed), typically along the length of the train [4,5,6]. Slipstream is proportional to the train's travelling speed, thus any increases in freight-train operational speeds, will result in the slipstream becoming more important. Some researchers have found that the loading configuration (wagons types, containers, gaps) have a large influence on a freight-train's slipstream [4,5,6]. However, the causal flow mechanism, and thus insight for potential informed aerodynamic optimisation is not well understood. There is therefore clear scope and motivation for improved understanding and subsequent optimisation of freight trains for improved slipstream performance.

## **2 Experimental Methodology**

In this work, the slipstream of freight trains was investigated using two experimental aerodynamic methodologies: a scaled wind-tunnel and scaled moving-model. This enables the effect of loading configuration on the slipstream of freight trains to be investigated with both high variability of parameters, large data sampling and flow field measurement in the wind tunnel experiment, as well as TSI-type gust analysis to be performed on individual measurement runs (representative of full-scale assessment) in the moving-model experiment.

### **2.1 Wind Tunnel Experiment**

The wind-tunnel experiments were performed in the "Side Wind Tunnel – Göttingen" SWG, illustrated in Figure 1. It is a closed test-section, return "Göttingen Type" wind-tunnel with a test section of 2.4 m wide, 1.6 m tall and 9 m long, and capable of freestream velocities up to ~60 m/s using a 0.5 MW fan. The wind-tunnel test-section was configured to testing the long freight train model, by adding a 0.45m splitter plate, that removes the artificial boundary layer (relative to real-world operation of a freight train in open air) that develops on the wind tunnel floor. The splitter plate was 8m long, and contained a scaled single-track ballast and rail (STBR) according to EN 14067-4: 2013+A1:2018.

The wind-tunnel model was a 1:15 reduced scale generic freight train (Fig. 1). It consisted of a generic nose with no discernable locomotive features, only smooth rounded surfaces so no specific aerodynamic features developed. The cross section of the train was 170 mm x 195 mm (2.55 m x 2.95 m in full-scale). The nose section 'upstream' in the wind tunnel, was 2.4m long and is important to influence the flow, so that the flow reaching the 'test-section' of the model is realistic, representative of flow around a real freight train. The 'test-section' of the model was 3.3 m length, which corresponds to 49.5 m in full-scale. This section is intended to be representative of the general 'middle' of a typical freight train, which in reality is representative of ~90% of a full train, beyond the local influence of the nose and tail of the train. In this section, the loading configuration can be varied, with a large variety of different container shaped elements, resulting in many different combinations of gap distances, number of gaps, and container lengths. After the test-section, 'downstream' in the wind tunnel, was a 0.5 m tail section. This was important to influence the flow after the test section in a realistic manner, so it leaves the test-section area in a realistic,

representative way as it would in a real, full-scale freight train. The model setup is illustrated in Figure 1, with photos in Figure 2.

The freight model has a generic wagon modelled, essentially a flat plate, 20 mm thick, and the same 170 mm width as the 1:15 scale container. Generic bogies are included, with wheels, triangular supporting elements, and an axle, in attempt to provide some realistic ‘roughness’ in the underbody region, disturbing the flow in this region to some extent. However, the focus of this experimental setup is to measure the impact changes in the container configuration has on the aerodynamic characteristics of a freight train.

Slipstream measurements were performed in the wind-tunnel experiment using 3, 5-hole *Vectroflow* dynamic-pressure probes. The probes have a 3mm diameter tip and are 120 mm long. The 5-hole probes were installed in a streamlined support structure (visible in Figures 1 & 2), at heights of  $z=13.3$ , 93.3 and 180 mm above top of rail (TOR) which correspond to the TSI measurement heights of 0.2 m and 1.4 m, with 2.7 m (approximately half container height) being included for further insight. They were positioned at 200 mm from track center, which corresponds to 3 m in full scale, being consistent with the TSI slipstream measurement position.

The test conditions of the wind tunnel were also measured, with atmospheric pressure in the test-hall, temperature, and freestream velocity being measured with a pitot-static tube installed in the roof (300 mm from the roof, above the upstream nose of the model). The 5-hole probes were traversed across 4m centered on the 3.3 m model test-section, with 25 mm spatial resolution, resulting in 161 data points per measurement. Samples were taken for 10 seconds at each point, at 2000 Hz sampling rate.

The flow field in the proximity of a single gap was also investigated at a freestream velocity of 50 m/s using Particle Image Velocimetry (PIV). The flow was seeded with particles and illuminated with two, 350 mJ/pulse laser sheets at 10 Hz located at  $z=0.93$  m (the TSI slipstream measurement height of 1.4 m), and captured with two, CMOS pco.edge 5.5 cameras. The interrogation window had an area of 750 mm x 320 mm total (from the two combined sheets). This resulted in the horizontal velocity (longitudinal and spanwise velocity components:  $u$  and  $v$ ) being captured every 1/10 seconds, with 5000 samples taken for each loading configuration.

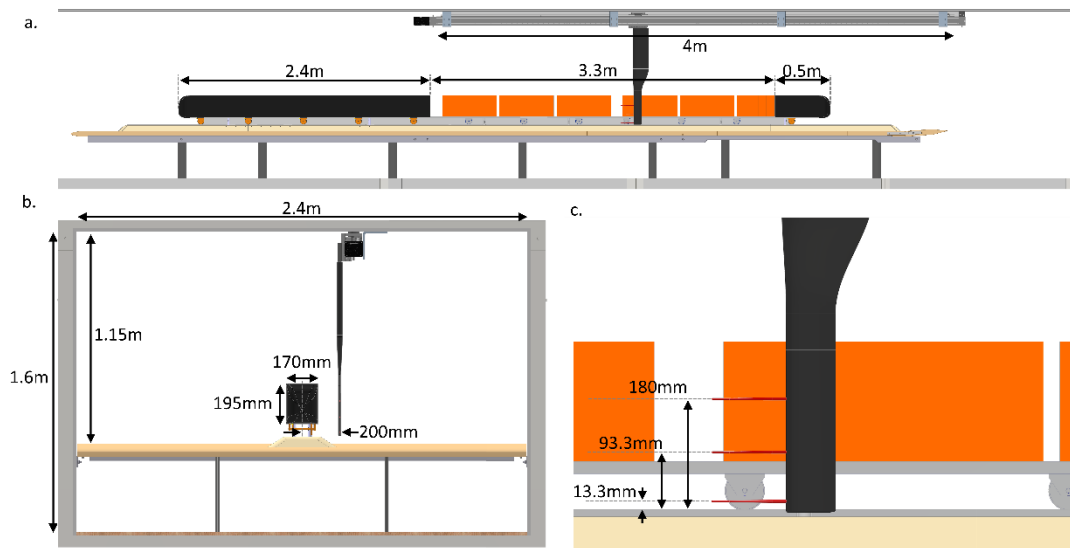


Figure 1: Wind-tunnel slipstream measurement setup diagram.



Figure 2: Wind tunnel slipstream measurement photos.

## 2.2 Moving Model Experiment

In the moving-model experiment, a freight train model is accelerated by a catapult mechanism up to 45 m/s (160 km/h). The model then coasts freely on functioning bogies across a rail, through a 23 m long test-section where measurements are made. After travelling 60 m, the model is decelerated in a braking tank filled with polystyrene balls. The moving-model facility, referred to as the Tunnel Simulation Facility – Göttingen (TSG), is illustrated in Figures 3-5 with photos presented in Figure 6.

The moving-model facility test-section was configured for slipstream specific measurements. In addition to the modelled ground – a flat 19 m long, 1.12 m wide plate – a scaled single-track ballast and rail (STBR), was included, according to EN 14067-4: 2013+A1:2018 [2], in the same manner as the wind-tunnel experiments. The STBR started at the front of the table, and was 12 m long.

A 1:22.7 scale, generic freight train was used. This model was developed by modifying an existing high-speed train (HST) model. The top 80% of the HST geometry was removed, and replaced with an in-house 3D printed geometry representative of a generic, idealized 2.7 m long model freight train. The front ‘upstream section’ was 1 m long, had the upper cross section of a 1:22.7 scale container (112 mm width, 120 mm height corresponding to 2.55 m and 2.75 m in full-scale), with elliptical upper and side edges to prevent any local flow features from occurring at the nose (which could have an effect downstream). Behind the nose section, was the 1.2 m long ‘test-section’ of the model, where the loading configuration could be varied with different container lengths and resulting gaps between them. This 1.2 m long model test-section corresponds to 27.24m full-scale, which was sufficient to model realistic loading configurations (including buffer distances upstream and downstream) on 52 ft. or 80 ft. wagons, capable of loading 2 or 3 swap bodies respectively. A 0.5 m tail section was behind the test-section, so the ‘test-section’, the area of interest for measurements, experienced representative airflow upstream and downstream. The cross-sectional area of the model was 0.0182 m<sup>2</sup>, corresponding to 9.115 m<sup>2</sup> in full scale.

The underbody, unlike an operational freight train, was fully covered, similar to a full aerodynamic fairing, and had curved lower corners, as it was the bottom of the existing HST model. This model underbody included generic bogies, each with 2 axles and wheels (that were functional for the model to roll across the rails). The bogies and wheels modelled in the moving-model experiment are more realistic and complex than in the wind-tunnel experiment, however, they are also largely shielded from airflow due to the underbody fairing.

The slipstream measurements were performed using hot-wire anemometry. Single, vertical hot-wire filaments were used, which directly measure the ‘horizontal’ velocity (longitudinal and spanwise flow relative to the train) generated by the vehicle’s movement through the stationary air. A total of 6 hot-wire probes were used in this experiment, 3 at 9 mm height and 3 at 62 mm height, corresponding to 0.2 m and 1.4 m above top of rail, the TSI full-scale measurement heights. These were all taken on one side of the model, and each probe was 1 m downstream from the next, with the measurement height alternating (so 2 m between each of the same-height probes). This 1 m distance corresponds to 22.7 m in full-scale, which is larger than the 20 m full-scale distance between probes recommended by the TSI and CEN regulations. This is to ensure multiple measurements can be taken of the same train passing / ‘run’ without the flow being correlated (same information being in the measurements).

The model velocity was determined by two pairs of 400 mm wide light-gates positioned at the start and end of the test-section plate. As the model passes through the light gates, the signal is changed, and the time difference between each of the pairs enables the velocity to be calculated. The facility test-section temperature and atmospheric pressure are also recorded, which were used to determine air density. Slipstream measurements were 3s long samples for each run, at a sampling frequency

of 20 kHz. The slipstream velocity is presented normalized by the model train speed,  $V_T$ , in the same manner as the wind-tunnel results.

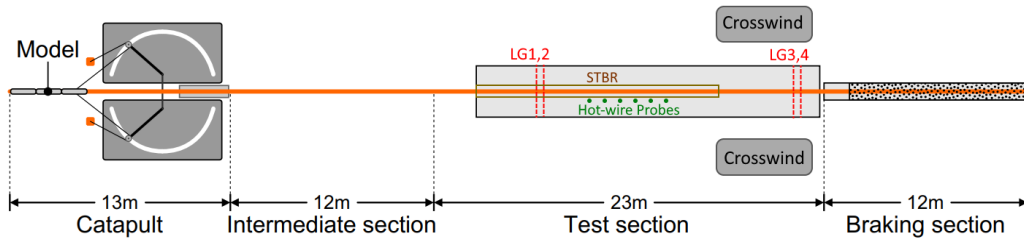


Figure 3: TSG (Tunnel-Simulation facility Göttingen) moving-model facility in slipstream measurement configuration.

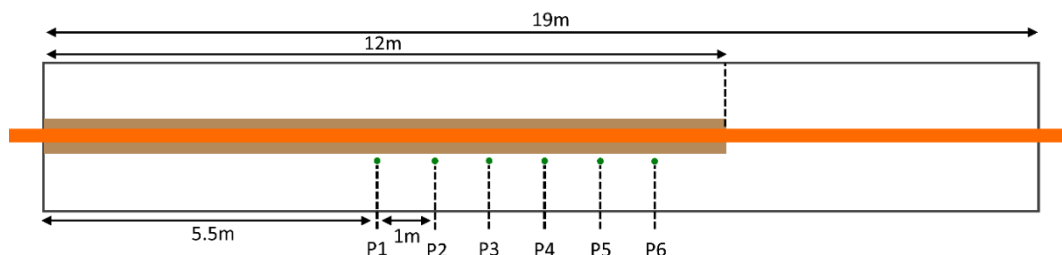


Figure 4: Moving-model slipstream measurement setup.

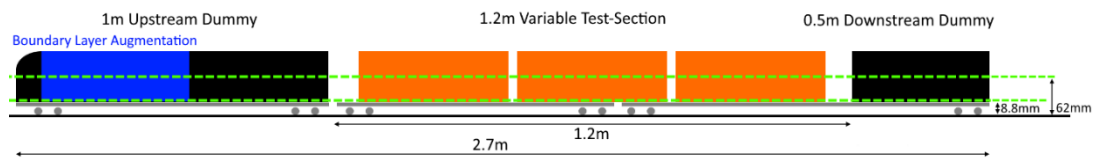


Figure 5: Moving-model setup.



Figure 6: Moving-model slipstream measurement photos.

### 2.3 Test Loading Configurations

A variety of different loading configurations, representative of ‘realistic’ operational configurations based on 24 ft. and 26 ft. swap body containers (7.45 and 7.82 m long respectively) loaded on a representative 80 ft. wagon, and a 52 ft. wagon, capable of loading 2 or 3 swap bodies respectively, were investigated in both experiments. These are illustrated in Figures 7 and 8. The configurations also included potential interesting combinations from an aerodynamic perspective. The corresponding

configurations range from fully loaded, missing container(s), resulting in container-container (0.6-0.8 m), wagon-wagon (1.4-1.8 m) and container (>7.45 m), sized gaps. The colours used for each configuration in the Figures 7,8 and the respective slipstream figures are comparable for both wind-tunnel and moving-model experiments.

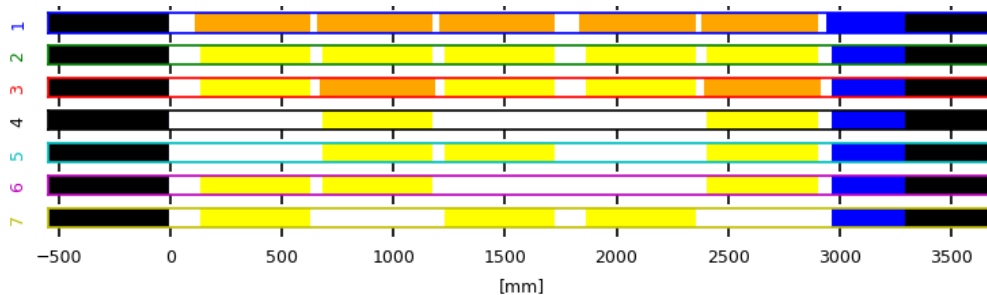


Figure 7: Wind-tunnel loading configurations tested

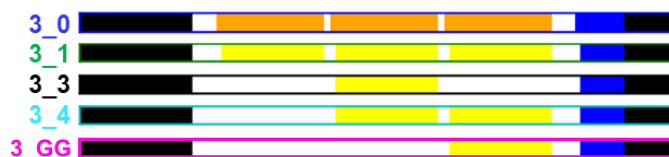


Figure 8: Moving-model loading configurations tested

### 3 Results

#### 3.1 Wind Tunnel

Examples of the slipstream measurements in the wind tunnel experiment are presented below in Figure 9 for two loading configurations; Scenario 0 (fully loaded) and scenario 3 (2 missing containers). The longitudinal,  $U$ , and horizontal,  $V$ , velocity components presented, as well as the resultant velocity of  $U$  and  $V$ , marked here as  $V_{UV}$ . According to TSI, only the horizontal velocity components are evaluated [1], for this reason, the vertical velocity  $w$  is not shown. Slipstream velocity, experienced in a ground-fixed frame of reference in the real-world,  $U_{GF}$ , is derived from the train-fixed frame-of-reference measurements in the wind-tunnel  $U_{TF}$ , by calculating the deficit in the freestream velocity,  $U_0$ , thus:  $U_{GF}=U_{TF}-U_0$ . The ground-fixed component,  $U_{GF}$  is the component contributing to  $V_{UV}$  calculation.

In Figure 9, an increasing deficit from freestream velocity is visible in  $U_{GF}$  along the length of the model, thus increasing slipstream velocity in the longitudinal velocity, as well as local peaks in the horizontal velocity near the container gaps. This corresponds to an overall increasing slipstream velocity profile with specific characteristics based on the loading configuration. The profiles of standard deviation in Figure 9 show similar characteristics, with higher fluctuations at peak slipstream velocities caused by the loading configuration. The standard deviation presented here, is based on the time-signal with a 1/15s moving-average first applied, equivalent to the 1s moving-average applied to signals measured in full-scale. The final profile in

Figure 9 is the mean + 2 times standard deviation ( $V_{UV}+2\sigma_{UV}$ ), this gives an indication on the peak slipstream velocities, analogous to the gust analysis performed in moving train/model experiments for TSI assessment.

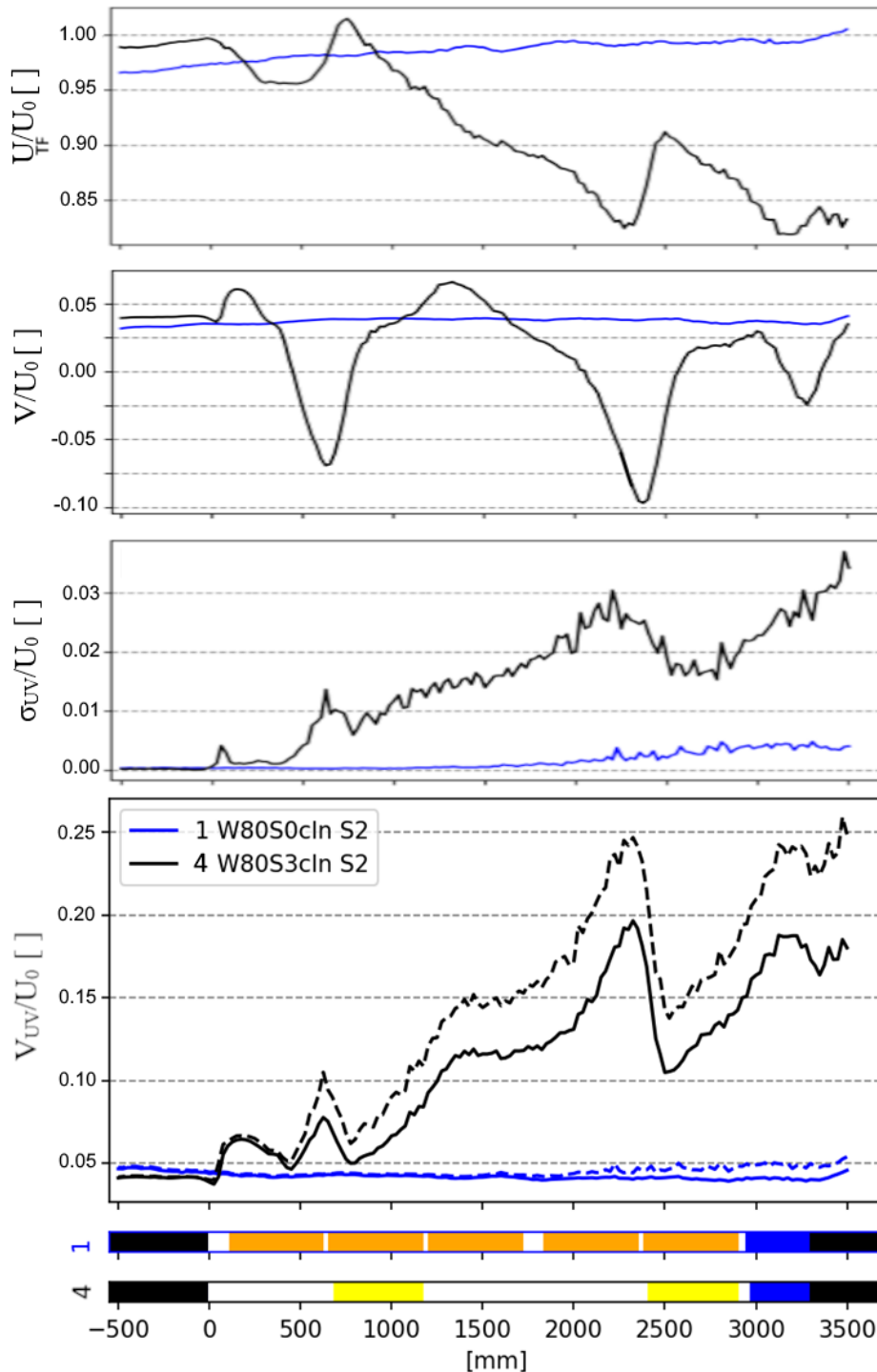


Figure 9: Slipstream profiles of  $U_{TF}$ ,  $V$ ,  $\sigma_{UV}$ , and  $V_{UV}$  with  $V_{UV}+2\sigma_{UV}$  as dashed lines for example loading configurations 1 and 4.



In Figure 10, the peak slipstream velocities for different realistic loading configurations are presented. In general, a trend exists across the three different measurement heights. For the ‘smooth’ loading configurations 1,2,3, the slipstream velocity clearly decreases with increasing height. For the ‘rough’ configurations 4,5,6,7 with at least one missing container, the large gap’s specific effect is clearer at higher measurement positions. This can be expected to be due to the local effect of the wagon geometry (wheels, axles, and horizontal plate that the container is loaded onto) which is basically in line with the lowest measurement position. Thus, slipstream measured at the lower position measures the influence of the wagon and the ~boundary layer growth that builds on this area. In contrast, the higher positions are progressively more influenced by the container gaps, which are spatially closer to these measurement positions, and contribute more directly to the slipstream profile.

The effect of the different loading configuration on the slipstream is significant. Large gaps (7.45-7.82 m), caused by missing container/empty slot, results in local effects on the slipstream profile, and subsequently lead to peak slipstream velocities by the end of the test-section of the freight model. The ‘rougher’ configurations 4,5,6,7 with one or more empty container gaps, have peak slipstream of 0.15-0.25 in contrast to the 0.05-0.1 of the ‘smooth’ loading configurations 1,2,3, which have no container gaps. It is clear to optimize the slipstream performance of a freight train, removing container sized gaps, is the primary measure.

The size of gaps between wagons has a smaller but still noticeable effect on the slipstream. Configuration 1 is clearly lower than 2 and 3, where the difference is in the wagon-wagon gap (1.4-1.8 m). This can account for differences between the loading configurations with the similar configurations. Configurations 5 and 7 both have two large gaps, but 7 also includes an additional larger wagon-wagon gap, resulting in higher overall relative slipstream. In contrast, container-container gap within a wagon (0.6-0.8m) makes negligible difference; configurations 2 and 3 have similar slipstream characteristics, with different container-container gaps.

The results also display sensitivity to both gap order, and potential cumulative effects. Configuration 4, with 3 missing containers isn’t significantly higher than configurations 5 and 7 which have similar peak slipstream magnitudes and only 2 missing containers. Configuration 6, with two gaps together, exhibits consistently lower slipstream than configurations 5,7, which have two, separated gaps. A possible explanation here is that two gaps together present such a large space, that the flow is essentially able to ‘reset’ to an extent, rather than build upon its previous disturbances. Both configurations 5 and 7 have repeated individual gaps, where the change in slipstream profiles are different for the first gap to the second. The individual gap doesn’t have the same incremental change to average or standard deviation of velocity, its impact is dependent on what happened before it, it is a function of the cumulative effects of the other gaps. This phenomenon has also been observed in literature, where in full-scale and scaled experiments have shown that the slipstream of a freight train specifically doesn’t continue to increase [4,5,6]. Slipstream appears to eventually approach a level of equilibrium, where the flow is essentially saturated,

and individual gaps are no longer able to have a distinct, increasing effect, only manage to sustain the current level of slipstream.

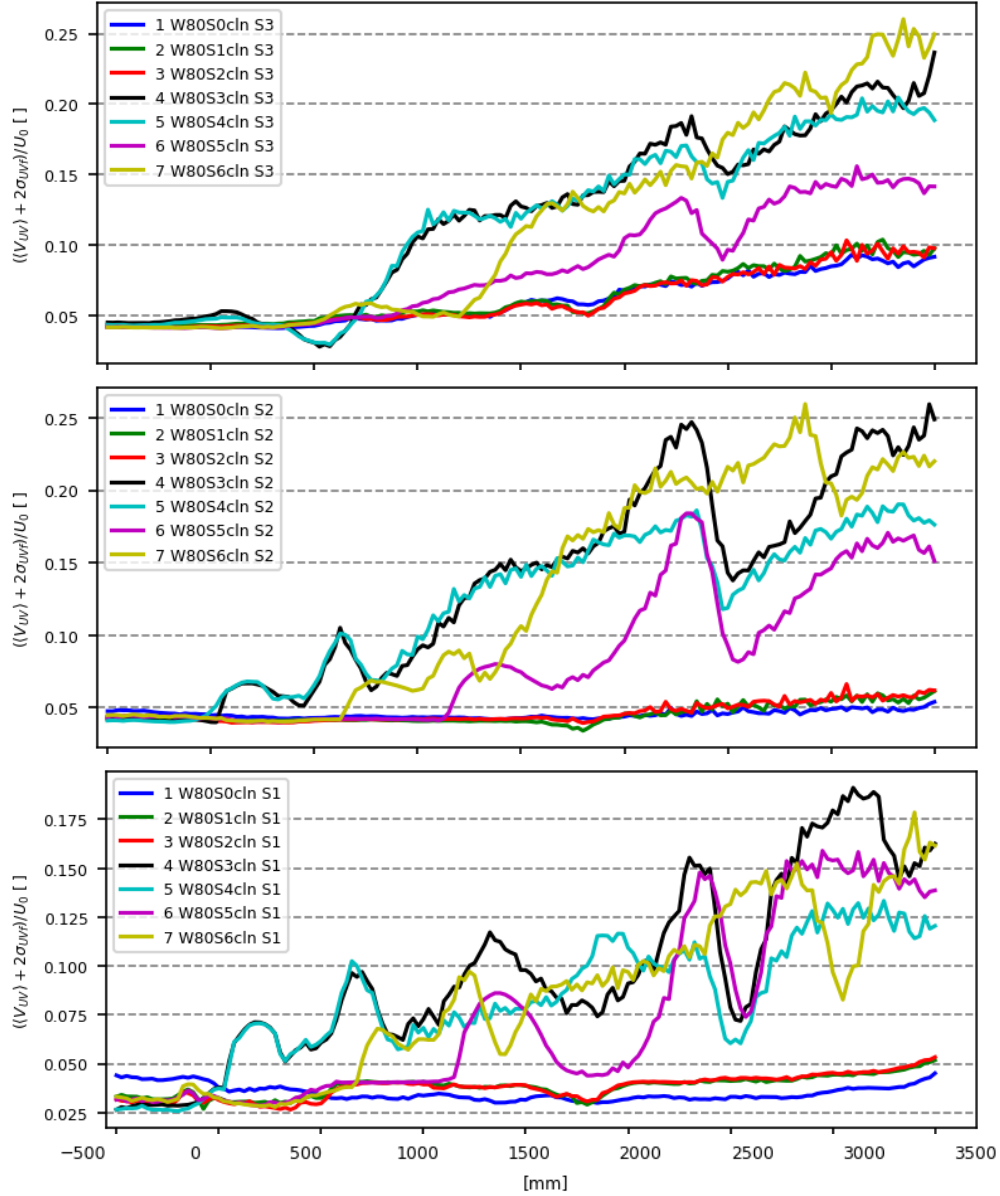


Figure 10: Peak slipstream velocity profiles  $V_{UV}+2 \sigma_{UV}$  for different loading configurations at 0.2 m (upper), 1.4 m (middle) and 2.7 m (lower).

### 3.2 Moving Model

Example slipstream results from the moving-model experiments for a ‘rough’ scenario 3 (two large individual gaps) are presented in Figure 11. The individual velocity profiles from the transient 21 ‘runs’ (in reality, 7 repeated runs, measured three times at each height), are illustrated, as well as the ensemble mean, std. dev. and mean+2 x std. dev. profiles. In Figure 11, the processing and resulting components

that make up the TSI value calculation are also illustrated for the rough loading configuration 3. Here, the velocity signal of each individual run is filtered with a spatial equivalent of 1s moving-average that is applied in full-scale (using an example full-scale operational velocity of 120 km/h). The maxima of each filtered individual run are highlighted as a point in the figure. Only maxima in the area affected by the loading configuration:  $x=0.75-4$  m are considered. The mean, standard deviation and mean plus two times the standard deviation of the individual maxima – the TSI value and its components – are presented as dashed lines in Figure 11.

The peak slipstream profiles for the 5 different realistic loading configurations tested in the moving-model experiment measured at  $z=0.2$  m and 1.4 m full-scale equivalent heights are presented in Figure 12, and the corresponding gust analysis and TSI values are presented in Table 1. These results confirm the findings of the wind-tunnel experiment, which was able to investigate a larger number of configuration variations. Namely, ‘rough’ configurations (3\_3, 3\_4 and 3\_GG) with large container size gaps have a significant effect, increasing slipstream velocity significantly when compared to the ‘smooth’ configurations 3\_0 and 3\_1.

Similarly to the wind-tunnel results, the order of the large gaps is also important on the overall peak slipstream magnitude achieved along the test-section of the model. In both experiments, double gaps have lower slipstream than two individual gaps. This is clearly visible in Figures 12, the 3\_GG profile at  $z=1.4$  m demonstrates the ability for the large double gap to partially ‘reset’ the overall increase in slipstream velocity, minimizing the overall level it increases to. In contrast, 3\_4 shows that two isolated gaps manage to perturb the flow, and incrementally increase the slipstream velocity. Another similarity to the wind-tunnel results is that the difference in smaller wagon-wagon gap size between 3\_0 and 3\_1 result in a non-negligible increase in slipstream velocity.

The slipstream magnitudes of the moving-model (0.05-0.32) are slightly higher than the comparable magnitudes of the wind-tunnel (0.05-0.3), but the relative loading configurations trends are consistent. Further, the greater sensitivity of the higher position to container gaps, with clearer characteristic signature of the container being visible at  $z=1.4$  m is also consistent between both experiments. The minor differences in the magnitudes of the slipstream profiles can potentially be attributed the differences in the model-wagon geometries of the two experiments.

<b>Configuration</b>	<b>Z=0.2 m</b>	<b>z=1.4 m</b>
<b>3_0</b>	0.077	0.047
<b>3_1</b>	0.094	0.106
<b>3_3</b>	0.254	0.320
<b>3_4</b>	0.253	0.271
<b>3_GG</b>	0.238	0.229

Table 1: TSI gust/peak slipstream values from the moving-model experiment.

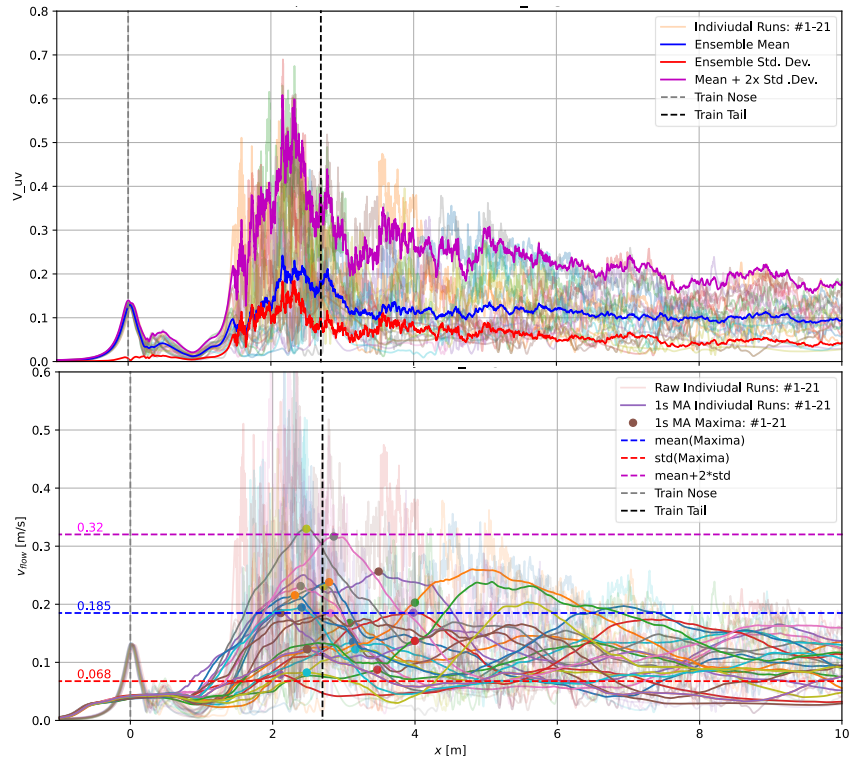


Figure 11: Individual measurements at  $z=1.4\text{m}$  for loading scenario 3\_3. Upper: individual and corresponding ensemble average, standard deviation profiles. Lower: Raw/filtered individual runs, maxima (points), TSI value/components (dashed lines).

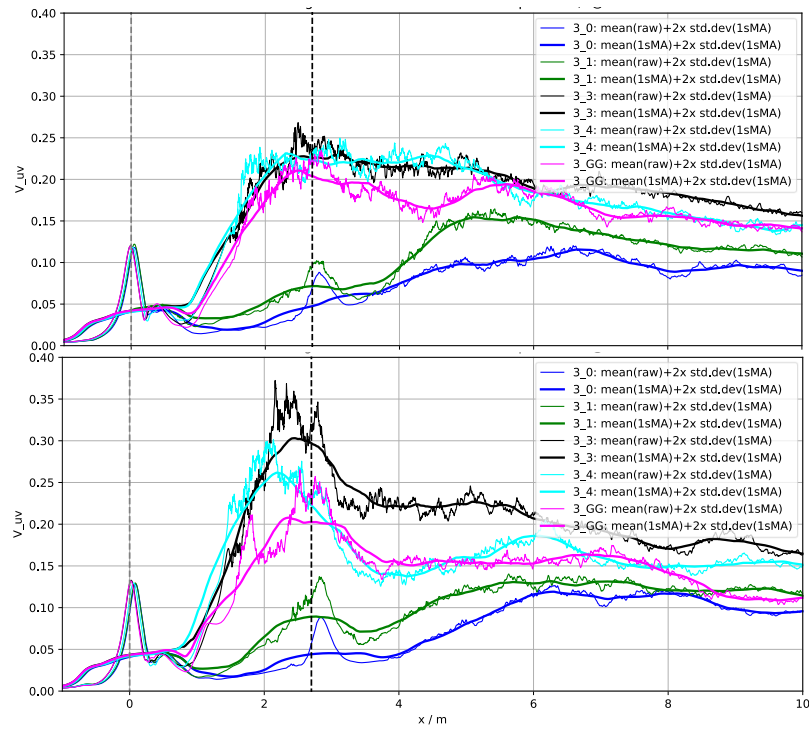


Figure 12: Ensemble averages for different loading configurations, at  $z=0.2$  (upper),  $1.4\text{ m}$  (lower).

### 3.3 Flow Field

The instantaneous flow fields of resultant slipstream velocity around two different container gap sizes: wagon-wagon (2 m), and container sized (7.8 m), are presented in this section. As identified in the instantaneous results from the moving-model experiment, as well as the high levels of velocity variation measured in the wind-tunnel experiment, the flow, even where the slipstream can be highest, also varies.

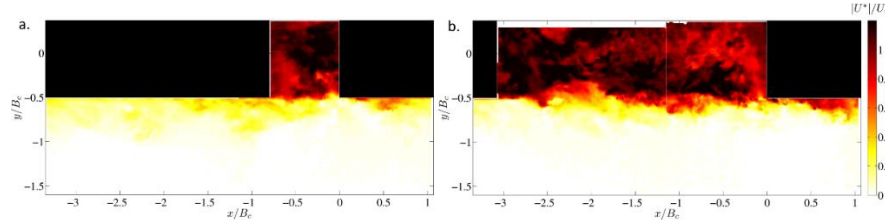


Figure 13: Contained instantaneous slipstream flow-fields. Left 2m, Right 7.8m gap.

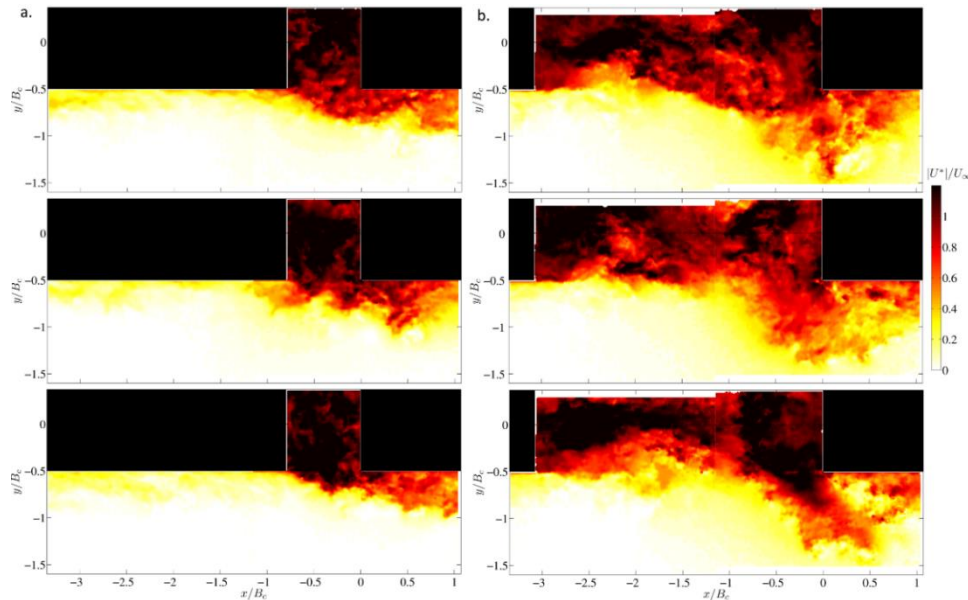


Figure 14: Deflected instantaneous slipstream flow-fields. Left 2m, Right 7.8m gap.

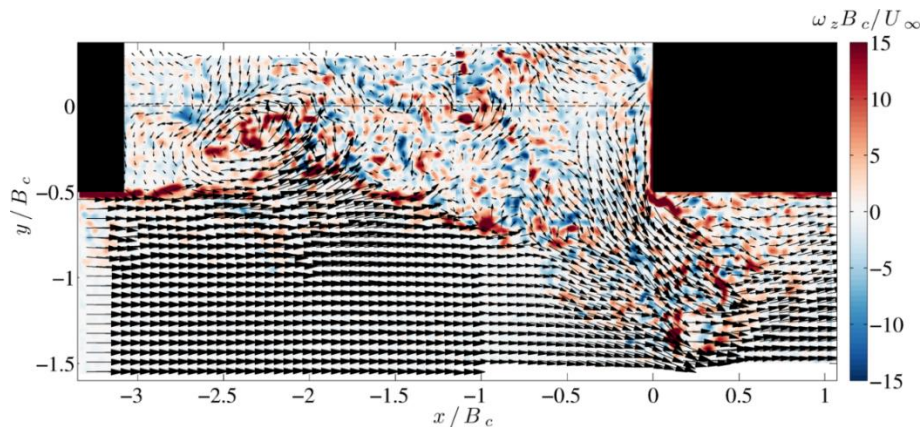


Figure 15: Deflected instantaneous slipstream: vectors and vorticity, 7.8 m gap.

In Figure 13, two example instantaneous snapshots of the flow field are presented for both gap sizes. Some slipstream velocity is apparent along the train sides, from the boundary layer. Significant induced flow is visible between the containers, but minimal flow moves beyond the width of the container; at this instant, low slipstream measurement occurs. In contrast, in three different instantaneous snapshots for each gap size, Figure 14 shows flow moving outwards from the container, and significantly further outwards for the larger gap size. Such flow field is the causal mechanism for slipstream peaks measured. This is elucidated in Figure 15, where the flow field is represented by velocity vectors and coloured with vorticity. Air moves inwards behind the first container, in this case forming a vortex, this results in more air reaching the forward-facing surface of the 2<sup>nd</sup> container, which then deflects the flow outwards.

## 4 Conclusions

The effect of loading configuration on the slipstream of freight trains has been investigated with both wind-tunnel and moving-model experiments. Strong agreement of slipstream magnitudes and trends between the moving-model and wind-tunnel experimental results was observed. Large, container-sized gaps (>7.45 m) were confirmed to generate a significant increase in slipstream, highlighting the potential for significant slipstream optimization by fully loading a freight train. Medium, wagon-wagon sized gaps (1.4-1.8 m) were observed to make secondary increase in slipstream, highlighting potential for optimization of this distance. Small, container-container gaps within a wagon (0.6-0.8 m) had a negligible difference. Flow field measurements identified the causal flow mechanism of slipstream peaks; unsteady entrainment behind the leading container, and outwards deflection of flow from the trailing container - leading to insight for future informed aerodynamic optimization.

## References

- [1] European Rail Agency (ERA), EU Technical Specification for Interoperability Relating to the 'Rolling Stock' Sub-System of the Trans-European High-Speed Rail System (HS RST TSI), 232/EC., 2008.
- [2] European Committee for Standardization. Railway Applications, Aerodynamics, Part 4: Requirements and test procedures for aerodynamics on open track, EN 14067-4: 2013+A1:2018
- [3] J.R. Bell, D. Burton, M.C. Thompson, A. Herbst, J. Sheridan "Moving model analysis of the slipstream and wake of a high-speed train", *Journal of Wind Engineering and Industrial Aerodynamics*, 166, 2017.
- [4] D. Soper, C. Baker, "A full-scale experimental investigation of passenger and freight train aerodynamics", *Proceedings of the Institution of Mechanical Engineers, Part F: Journal of Rail and Rapid Transit*, 232 (5), 2019.
- [5] D. Soper, C. Baker, M. Sterling, "Experimental investigation of the slipstream development around a container freight train using a moving model facility", *Journal of Wind Engineering and Industrial Aerodynamics*, 135, 2014.
- [6] J.R. Bell, D. Burton, M.C. Thompson, "The boundary-layer characteristics and unsteady flow topology of full-scale operational inter-modal freight trains", *Journal of Wind Engineering and Industrial Aerodynamics*, 201, 2020.